

Coincident occurrences of tropical individual cirrus clouds and deep convective systems derived from TRMM observations

Bing Lin^{*1}, Kuan-Man Xu¹, Patrick Minnis¹, Bruce A. Wielicki¹,
Yongxiang Hu¹, Lin Chambers¹, Alice Fan², and Wenbo Sun³

¹Sciences Directorate

NASA Langley Research Center

Hampton, VA 23681

²SSAI, One Enterprise Parkway

Hampton, VA 23666

³Hampton University, Dept. of Atmospheric and Planetary Sciences

Hampton, VA 23666

Prepared for Geophys. Res. Letter

January 2007

*Corresponding author's address: Dr. Bing Lin, MS 420, NASA Langley Research Center, Hampton, VA 23681-2199; email: bing.lin@nasa.gov; phone: 757-864-9823; fax: 757-864-7996.

Abstract

Measurements of cloud properties and atmospheric radiation taken between January and August 1998 by the Tropical Rainfall Measuring Mission (TRMM) satellite were used to investigate the effect of spatial and temporal scales on the coincident occurrences of tropical individual cirrus clouds (ICCs) and deep convective systems (DCSs). It is found that there is little or even negative correlation between instantaneous occurrences of ICC and DCS in small areas, in which both types of clouds cannot grow and expand simultaneously. When spatial and temporal domains are increased, ICCs become more dependent on DCSs due to the origination of many ICCs from DCSs and moisture supply from the DCS in the upper troposphere for the ICCs to grow, resulting in significant positive correlation between the two types of tropical high clouds in large spatial and long temporal scales. This result may suggest that the decrease of tropical high clouds with SST from model simulations is likely caused by restricted spatial domains and limited temporal periods. Finally, the radiative feedback due to the change in tropical high cloud area coverage with sea surface temperature appears small and about -0.14 Wm^{-2} per degree Kelvin.

1. Introduction

Tropical high clouds not only have strong influences on atmospheric radiation but also are one of driving factors for the variations of tropical precipitation and upper tropospheric humidity with sea surface temperature (SST), as demonstrated by recent satellite observations (*Luo and Rossow* [2004], *Su et al.* [2006], *Lin et al.* [2006] and references therein). There is some evidence suggesting that tropical high clouds may enhance the greenhouse effect through a positive water vapor feedback in warm climates [*Su et al.*, 2006]. Although much effort has been made to evaluate climate feedbacks of the high clouds from observations (e.g., *Ramanathan and Collins*, 1992; *Wallace*, 1992; *Fu et al.*, 1992; *Hartmann and Michelsen*, 1993, 2002; *Lin et al.*, 2002; *Chambers et al.*, 2002; *Lindzen et al.*, 2001; *Del Genio and Kovari*, 2002), quantitative and accurate estimates of climate feedbacks of these tropical clouds are still limited. Understanding the variations of these high clouds with SST is a critical first step to accurately estimate their climate feedbacks.

There are generally two types of tropical high clouds: deep convective systems and individual cirrus clouds. A deep convective system (DCS) is a contiguous high cloud sheet with embedded active deep convective cores, and an individual cirrus cloud (ICC) is a tropical high cloud patch without any deep convective cores or simply any high clouds not belonging to a DCS. Because tropical convection is strongly organized, most tropical high clouds are DCSs [*Lin et al.*, 2006]. ICCs can be composed of dissipated DCSs, newly developing convective systems without surface precipitation, or locally developed in-situ cirrus clouds [*Luo and Rossow*, 2004]. Both DCS and ICC are important contributors to climate sensitivity due to their influences on upper tropospheric humidity and the radiation balance. There are, however, considerably different interpretations of their roles in climate feedbacks. For example, *Lindzen et*

al. [2001] suggested that the areal coverage of these tropical high clouds decreases with increasing temperature due to the effective removal of the moisture to be transported to the upper troposphere by increased precipitation and precipitation efficiency. *Ramanathan and Collins* [1992] and *Del Genio and Kovari* [2002] indicated that more tropical high clouds form in warmer climates due to enhanced convection. Results from cloud resolving model simulations with limited domain sizes and time periods showed that the column cloud fractions are slightly reduced as SST increases [*Tompkins and Craig*, 1999; *Wu and Moncrieff*, 1999; *Eitzen and Xu*, 2007], but the upper-tropospheric cloud fractions increase as SST rises [*Tompkins and Craig*, 1999; *Eitzen and Xu*, 2007].

Recently, *Lin et al.* [2006] investigated the DCS type of tropical high clouds using measurements from the Tropical Rainfall Measuring Mission (*TRMM*) satellite data during Clouds and the Earth's Radiant Energy System (*CERES*) *TRMM* period (January — August 1998) and found that the DCS areal coverage increases with SST despite the increases in both DCS precipitation and rainfall efficiency with SST. Higher sea surface temperature result in enhanced boundary layer moisture and the moisture transported into the upper troposphere. The increased transports of moisture available for cloud formation, along with changes in the cloud formation efficiency, likely contribute to the significant increase of DCS area coverage with SST.

This study focuses on observations of the ICC type of tropical high clouds, especially the coincident occurrences of ICC and DCS using *TRMM* satellite measurements. The effects of temporal and spatial scales on the coincident occurrences of ICC and DCS are discussed. Section 2 introduces the data sets and analysis methods used in this study. Section 3 shows the

results. Radiative feedbacks of these observed clouds on climate and summary are given in section 4.

2. Data Analysis

Similar to our previous study [Lin *et al.*, 2006], this investigation analyzes *TRMM* data taken over oceans between 30°N and 30°S during January through August 1998. The time period is determined by CERES data availability. The CERES *TRMM* observations captured a transition from a strong El Niño during early 1998 to normal or weak La Niña tropical climate conditions, which includes large dynamic and thermodynamic changes needed to examine variability in the development of deep convection. The profound variations in the large-scale circulations and small-scale convective activities during this period also provide us a good chance to evaluate interrelationships of tropical high clouds at different scales. This paper focuses on the coincident occurrences of ICC and DCS. Measurements from three instruments on board the *TRMM* satellite: the CERES cross-track scanner, the Visible and Infrared Scanner (VIRS), and the *TRMM* Microwave Imager (TMI), are used in this study. The CERES scanner measures broadband shortwave (SW) and longwave (LW) radiation at a spatial resolution size of about 10 km, while the VIRS monitors narrow spectral visible (VIS), near-infrared, and infrared (IR) measurements at a nominal 2-km resolution over a 720-km swath. The TMI is used to detect precipitation and estimate precipitation intensity. TMI pixel sizes vary with frequency, from about 4.6 km × 7.2 km to 9.1 km × 63.2 km over a total swath width of 780 km.

The basic data set is the CERES single scanner footprint (SSF) product [Geier *et al.*, 2003]. Because the CERES product collocates CERES broadband measurements with CERES narrowband cloud retrievals from VIRS, the uncertainties in CERES SW and LW radiative flux

estimates are about a factor two smaller than those from the Earth Radiation Budget Experiment [Barkstrom *et al.*, 1989]. The SST data used in this analysis, from the Reynolds SST analysis [Reynolds and Smith, 1994], are included in the SSF product.

The CERES project, using a VIS-IR-Solar-IR-Split-window technique (VISST [Minnis *et al.*, 2002]), processes VIRS measurements to detect cloudy and clear skies, and to estimate bulk cloud properties, such as effective cloud top temperature (T_c) and height, cloud fraction, cloud thermodynamic phase, and cloud microphysical properties. The CERES cloud properties derived from 2-km resolution VIRS pixels are convolved into TMI 37-GHz field-of-views (FOVs) as in Ho *et al.* [2003] to minimize spatial and temporal collocation errors. Rainfall rate data from the Goddard level-2 standard TMI products [Kummerow *et al.*, 2001] are registered to the collocated data.

After collocating the CERES cloud products from VIRS with the TMI passive microwave measurements, we further match the data with the CERES SW and LW flux data. Since the FOVs of the TMI 37-GHz microwave measurements and CERES radiative flux observations are similar in size, their footprints usually do not have closed convolutions. Weighted matches are used to merge CERES with TMI data. , All CERES measurements within a 15-km radius of the center of each TMI tropical high cloud FOV are considered as matched CERES footprints. The average SW and LW fluxes for the matched CERES footprints, weighted by their proximity to the TMI FOVs, are calculated to represent the radiative properties of the high clouds that are covered by the TMI FOV.

To use *TRMM* data in detecting and analyzing tropical high clouds, we first search for a DCS, which includes at least one cold precipitating cell, within the combined *TRMM* data, as discussed in Lin *et al.* [2006]. All other tropical clouds with ice thermodynamic phase and IR (11

μm) brightness temperatures less than 270 K or cloud tops higher than 5 km are considered as ICCs. Key advantages of this study that were not available before the *TRMM* era are the use of TMI rainfall and VIRS thermal channel brightness temperature data together for DCS convective core detection and the combination of VIRS narrowband with CERES broadband data for the evaluation of the radiative effects of individual tropical high cloud types.

3. Results

The interactions among tropical high clouds, moisture fields and radiation are very complicated processes. The frequency and areal coverage of high clouds, hereafter cloud frequency, are related to many environmental parameters, as shown by *Luo and Rossow* [2004] and *Lin et al.* [2006]. The present study mainly focuses on the effects of temporal and spatial scales on the coincident occurrences of two different types of the tropical high clouds, namely ICC and DCS. We will first show the analysis of their frequencies of occurrences at instantaneous and small spatial ($1^\circ \times 1^\circ$) scales and then gradually extend the analysis to longer (inter-seasonal) temporal and larger ($30^\circ \times 30^\circ$) spatial scales. The tropical high cloud radiative feedbacks are estimated based on the observed variability of the high clouds, which will be discussed in section 4.

Figure 1 shows scatter plots of 36-hour composite cloud frequencies of ICCs and DCSs in spatial domains from $1^\circ \times 1^\circ$ (upper left), $2.5^\circ \times 2.5^\circ$ (upper right), $5^\circ \times 5^\circ$ (lower left) to $10^\circ \times 10^\circ$ (lower right) for the entire tropics ($\pm 30^\circ$ latitudes) during January 1998. The 36-hour composites are used because at this temporal resolution, *TRMM* measurements almost cover the entire tropics and generally have no multiple observations at a single location, while at smaller time intervals, such as 24 hours, significant parts of the tropics are not scanned by the *TRMM*

satellite. Thus, the observations at this time scale can be considered as instantaneous measurements. It can be seen from the figure that at the smallest spatial scale ($1^\circ \times 1^\circ$), statistically, the frequencies of ICCs and DCSs are significantly negatively correlated. In a small area, more deep convection would generate more organized high clouds and suppress individual cirrus to develop simultaneously in the same area. This negative correlation is thus expected since the sum of the ICC and DCS frequencies cannot exceed 100%. When the spatial domain increases from $2.5^\circ \times 2.5^\circ$ to $10^\circ \times 10^\circ$, the negative correlation between ICC and DCS frequencies remains for high DCS frequencies, but a positive correlation begins developing for a range of small DCS frequencies, resulting in an insignificant correlation for the full range of DCS and ICC frequencies. At very large spatial scales (e.g., $30^\circ \times 30^\circ$), the ICC occurrences are mainly dependent on the large-scale dynamics and thermodynamics of the tropics, and moisture availability in the upper troposphere, which, as discussed by *Lin et al.* [2006], is part of the climate effects of DCS. Thus, the ICC frequencies have a slightly positive correlation with their DCS counterparts, as shown in Fig. 2, related to the disappearance of the scatter in the high DCS frequency range. Note that similar results to those shown in Figs. 1 and 2 are obtained for other months.

The transition behavior for the relationships of ICC and DCS from small to large spatial scales in the instantaneous data can also be found in long temporal (8-month) composites of the satellite measurements. But from the temporal perspective, only positive relationships between ICC and DCS are observed (Fig. 3), due to the elimination of weather noise from temporal variations of dynamics. The strong coincident occurrence of ICC and DCS at the longer time scales, especially when the spatial domain is very large (e.g. $30^\circ \times 30^\circ$ grid boxes), reflects the climatological dependence of cirrus clouds on convection for their origination and moisture

supply in the upper troposphere. The main reason for the different results from those shown in Fig. 1 is that climatic signals are the main contributor to the results shown in Fig. 3 while the variations caused by weather systems dominate the results shown in Fig. 1. These climatic signals modulate the occurrences of both types of tropical clouds, which also explain the higher positive correlations for the larger spatial regions shown in Fig. 3.

Further evidence of coincident occurrences of ICC and DCS can be seen from binned data. Figure 4 shows the means of ICC (+), DCS (*) and total high cloud (Δ) areal coverage for each 1K-SST interval using the 8-month dataset for the entire tropics. The variation of ICC directly follows that of DCS. As discussed by *Lin et al.* [2006], the total tropical high cloud cover is dominated by DCS. Although ICC only contributes a small fraction (about 5~10%) of the high clouds, their influence on climate, especially on the radiation balance, cannot be neglected. The averaged increase rate of high (ICC and DCS) clouds with SST is about 2.8% per degree Kelvin, slightly higher than that for DCS alone obtained by *Lin et al.* [2006].

4. Discussions and summary

This study uses the measurements taken during January through August 1998 from multiple *TRMM* sensors, namely CERES, TMI and VIRS, to evaluate the relationship between ICCs and DCSs and the radiative effects of tropical high clouds. The measurements from *TRMM* satellite show that relating occurrences (or areal coverage) of ICCs to those of DCSs in small domains is limited because large extended instantaneous DCSs tend to fill most of the domain and to suppress ICCs precluding a reliable assessment of the ICCs. When the spatial or temporal domains are increased, it becomes clear that the ICCs depend on DCS coverage due to the origination of the ICC from the DCS and its accompanying moisture supply in the upper

troposphere that maintains and grows the ICC. This results in significant positive correlations between the two types of tropical high clouds in large spatial and long temporal scales. This result suggests that the decrease of tropical high clouds with SST from model simulations [Tompkins and Craig, 1999; Wu and Moncrieff, 1999; Eitzen and Xu, 2007] is likely caused by the restricted spatial domains and perhaps limited simulation time periods used in these studies. However, the dynamic states were fixed in these SST sensitivity simulations, while the dynamic states in the observations might be slightly different for different SSTs.

Based on our observations it is not surprising to conclude that individual cirrus clouds climatologically vary consistently with deep convective clouds, and would not decrease with increase of deep convective clouds when the tropics get warmer, which contradicts some suggestions of dehydrate processes. The increase of high clouds with SST would produce certain climate radiative effects (i.e., feedbacks). Because high clouds may not be developed from a clear sky background, the commonly defined cloud radiative forcing, which is the radiative differences between cloudy and clear skies, cannot represent actual radiation change well. To estimate high cloud radiative feedback, this study follows the idea of generalized radiative forcing of tropical high clouds [Lin *et al.*, 2006], which defines radiative forcing as the difference between high clouds and existing environmental conditions. These existing environmental conditions could include low and middle clouds, moist, or partially cloudy conditions, but not the skies with high clouds.

The procedures for calculating the radiative effects from CERES measurements for tropical high clouds including both DCSs and ICCs are the same as those for DCS alone and can be found in Lin *et al.* [2006]. The average net high cloud radiative forcing from environmental conditions after weighting by the distribution of high clouds on SST is relatively weak (-4.95

W/m^2) only slightly more than 1/3 of the radiative forcing computed relative to clear conditions. Since the average increase of tropical high cloud areal coverage with SST is about 2.8%/K, the radiative feedback due to a change in high cloud areal coverage is about $2.8\%/K \times (-4.95 \text{ W/m}^2) = -0.14 \text{ W/m}^2/\text{K}$, which may be small compared to an anthropogenic forcing of doubled atmospheric CO_2 . This result suggests that the negative feedbacks of tropical high clouds are not likely to cancel the influence of increased atmospheric greenhouse gases on the climate. In addition to tropical high clouds, investigations of other types of clouds such as subtropical boundary-layer clouds are critical for overall understanding of cloud climate feedbacks and for improving predictions of future climate.

Acknowledgment. The authors would like to express their appreciation to G. Gibson, A. Cheng, D. Young, and Y. Luo for their valuable comments. This study was supported by NASA's Science Mission Directorate through the EOS data analysis and radiation science programs, the CERES mission, and the NASA Energy and Water cycle Studies (NEWS) program. CERES and VIRS products and TMI data were obtained from the NASA Langley Atmospheric Sciences Data Center in Hampton, Virginia and Goddard Distributed Active Archive Center in Greenbelt, Maryland, respectively.

References

- Barkstrom, B. R., E. Harrison, G. Smith, R. Green, J. Kibler and R. Cess (1989), Earth radiation budget experiment (ERBE) archival and April 1985 results, *Bull. Amer. Meteor. Soc.*, 70, 1254-1262.
- Chambers, L., B. Lin, and D. Young (2002) New CERES data examined for evidence of tropical iris feedback, *J. Climate*, 15, 3719-3726.
- Del Genio, A.D. and W. Kovari (2002), Climatic properties of tropical precipitating convection under varying environmental conditions, *J. Climate*, 15, 2597-2615.
- Eitzen, Z. A., and K.-M. Xu (2007) Sensitivity of a large ensemble of tropical convective systems to changes in the thermodynamic and dynamic forcings. *J. Atmos. Sci.*, (submitted).
- Fu, R., A. DelGenio, B. Rossow, and W.T. Liu (1992), Are cirrus clouds a “thermostat” for tropical sea surface temperature? *Nature*, 358, 394.
- Geier, E. B., R. N. Green, D. P. Kratz, P. Minnis, W. F. Miller, S. K. Nolan, and C. B. Franklin (2003), Clouds and the Earth’s Radiant Energy System Data Management System Single Satellite Footprint TOA/Surface Fluxes and Clouds (SSF) Collection Document, Release 2, Version 1. 243 pp. (http://asd-www.larc.nasa.gov/ceres/collect_guide/SSF_CG.pdf).
- Hartmann, D.L. and M.L. Michelson (1993), Large-scale effects on the regulation of tropical sea surface temperature, *J. Climate*, 6, 2049-2062.
- Hartmann, D. L., and M. L. Michelsen (2002), No evidence for iris, *Bull. Amer. Meteor. Soc.*, 83, 249-254.

- Ho, S.-P., B. Lin, P. Minnis, and T.-F. Fan (2003), Estimation of cloud vertical structure and water amount over tropical oceans using VIRS and TMI data, *J. Geophys. Res.*, *108 (D14)*, 4419, doi:10.1029/2002JD003298.
- Lin, B., B. Wielicki, L. Chambers, Y. Hu, and K.-M. Xu (2002), The Iris hypothesis: A negative or positive cloud feedback? *J. Climate*, *15*, 3-7.
- Lin, B., B. Wielicki, P. Minnis, L. Chambers, K.-M. Xu, Y. Hu, and A. Fan (2006), The effect of environmental conditions on tropical deep convective systems observed from the TRMM satellite, *J. Climate*, *19*, 5745-5761.
- Luo, Z. and W. Rossow (2004), Characterizing tropical cirrus life cycle, evolution, and interaction with upper-tropospheric water vapor using Lagrangian trajectory analysis of satellite observations, *J. Climate*, *17*, 4541-4563.
- Lindzen, R.S., M.-D. Chou, and A. Hou (2001), Does the Earth have an adaptive infrared iris? *Bull. Amer. Meteor. Soc.*, *82*, 417-432.
- Minnis, P., and co-authors (2002), A global cloud database from VIRS and MODIS for CERES. *Proc. SPIE 3rd Intl. Asia-Pacific Environ. Remote Sensing Symp. 2002: Remote Sens. Atmos., Ocean, Environ., and Space*, Hangzhou, China, October 23-27. (<http://www-pm.larc.nasa.gov/ceres/pub/conference/Minnis.SPIE.02.pdf>).
- Ramanathan, V., and W. Collins (1991), Thermodynamic regulation of ocean warming by cirrus clouds deduced from observations of the 1987 El Nino, *Nature*, *351*, 27-32.
- Reynolds, R.W., and T.M. Smith (1994), Improved global sea surface temperature analysis, *J. Climate*, *7*, 929-948.

- Su, H., W. G. Read, J. H. Jiang, J. W. Waters, D. L. Wu, E. J. Fetzer (2006), Enhanced positive water vapor feedback associated with tropical deep convection: New evidence from Aura MLS, *Geophys. Res. Lett.*, *33*, L05709, doi:10.1029/2005GL025505.
- Tompkins, A. M., and G. C. Craig (1999), Sensitivity of tropical convection to sea surface temperature in the absence of large-scale flow, *J. Climate*, *12*, 462-476.
- Wallace, J. (1992), Effect of deep convection on the regulation of tropical sea surface temperature, *Nature*, *357*, 230-231.
- Wu, X., and M. W. Moncrieff (1999), Effects of sea surface temperature and large-scale dynamics on the thermodynamic equilibrium state and convection over the tropical western Pacific, *J. Geophys. Res.*, *104*, 6093-6100.

Figure captions

Fig.1 Scatter plots of 36-hourly composite cloud frequencies of individual cirrus clouds versus deep convective systems (DCS) for January 1998. Spatial domains for the analysis increase from $1^{\circ} \times 1^{\circ}$ (upper left), $2.5^{\circ} \times 2.5^{\circ}$ (upper right), $5^{\circ} \times 5^{\circ}$ (lower left) to $10^{\circ} \times 10^{\circ}$ (lower right).

Fig. 2 Same as Fig.1, except for the data are composited for $30^{\circ} \times 30^{\circ}$ regions.

Fig. 3 Same as Fig. 1, except for data from 8 months of CERES TRMM measurements.

Fig. 4 Mean ICC (+), DCS (*) and total high cloud (Δ) areal coverage as a function of SST for the entire tropics, January - August 1998.

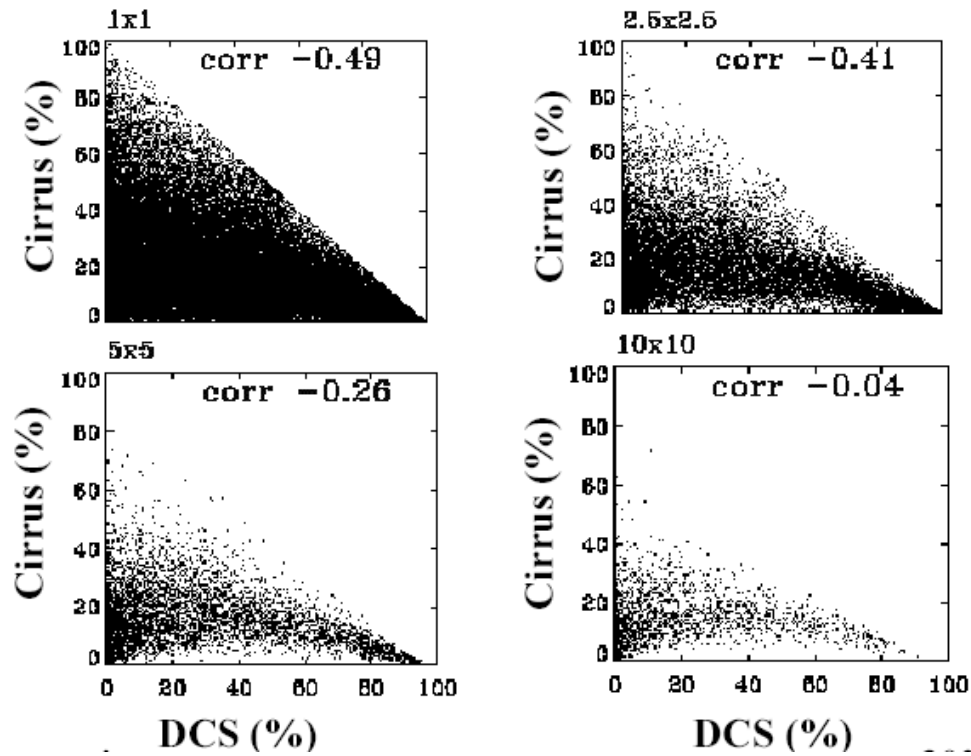


Fig. 1. Scatter plots of 36-hourly composite cloud frequencies of individual cirrus clouds versus deep convective systems (DCS) for January 1998. Spatial domains for the analysis increase from $1^\circ \times 1^\circ$ (upper left), $2.5^\circ \times 2.5^\circ$ (upper right), $5^\circ \times 5^\circ$ (lower left) to $10^\circ \times 10^\circ$ (lower right).

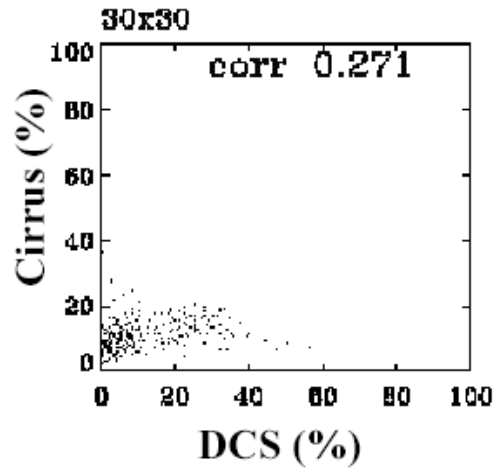


Fig. 2 Same as Fig.1, except for the data are composited for $30^{\circ}\times 30^{\circ}$ regions.

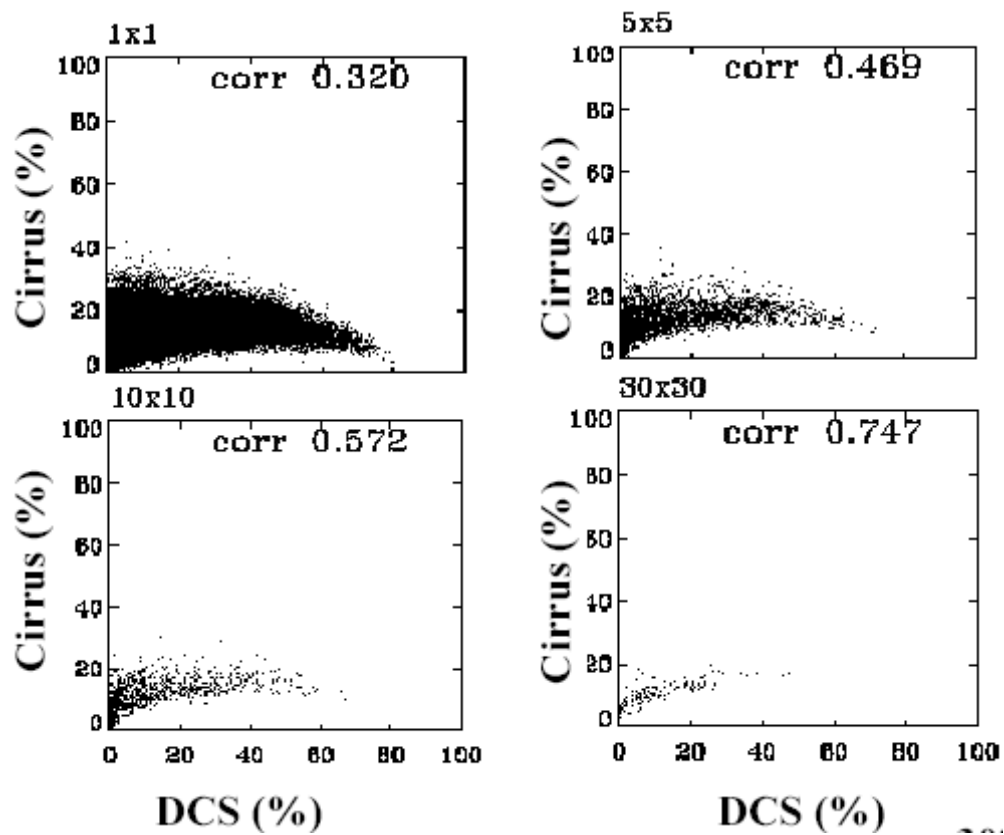


Fig. 3 Same as Fig. 1, except for data from 8 months of CERES TRMM measurements.

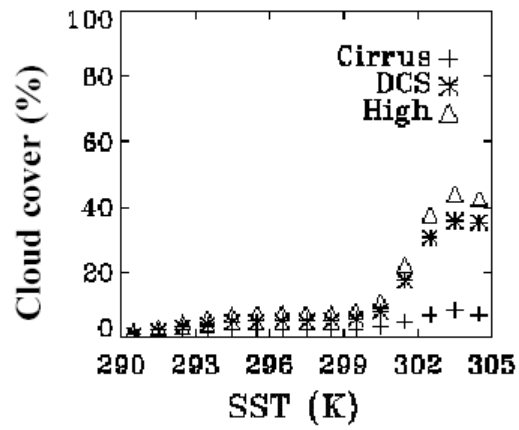


Fig. 4 Mean ICC (+), DCS (*) and total high cloud (Δ) areal coverage as a function of SST for the entire tropics, January - August 1998.